Radiochim. Acta **89**, 831–838 (2001)

Using ^{13}N as tracer in heterogeneous atmospheric chemistry experiments

By M. Ammann*

Paul Scherrer Institute, CH-5232 Villigen, Switzerland

(Received January 10, 2001; accepted in revised form June 20, 2001)

^{13}N / *Short-lived nuclides / PET / Nitrogen oxides / Aerosol / Atmospheric chemistry*

Summary. Current techniques aiming to study heterogeneous atmospheric chemistry under realistic conditions are often subject to restrictions caused by the low amount of processed material, the complex composition of gas and condensed phases and interference issues. The use of the short-lived tracer ^{13}N enables laboratory experiments pertaining to the atmospheric chemistry of nitrogen oxides to be performed at extremely low concentrations, ambient humidity and pressure. ^{13}N was produced through $^{16}O(p,\alpha)^{13}N$ reaction in a gas target in continuous mode, and transported as ^{13}NO in a carrier gas to the chemistry laboratory through a 70 m long capillary. Several gas-phase and surface chemical routines allowed converting ^{13}NO into other forms of oxidized nitrogen. Chemical separation and detection was achieved through chemically specific absorption reactions on the coatings of denuders, which additionally allowed separating gas-phase species from their particulate counterparts. In a first application, the reversible adsorption of NO_2 on a solid NaCl surface was investigated, from which an adsorption enthalpy of 28 kJ/mol was derived. As an example of a reaction with aerosol particles in gas suspension, the reaction of ^{13}N-labelled HNO_3 with sea-salt particles was studied using an aerosol flow reactor.

1. Introduction

Whereas atmospheric chemistry had been mainly dealing with gas-phase processes over the past 50 years, it has become clear over the past ten years, that the major remaining gaps of knowledge lie in heterogeneous chemistry in order to adequately describe the cycling of the most important trace constituents, the global and local ozone budget and the aerosol cloud climate interactions [1]. Our knowledge on heterogeneous chemistry, which in this context addresses all interactions between the gas-phase and condensed phases such as solid and liquid aerosols, clouds and ground surfaces, is still insufficient [2]. Because of the complexity of the systems involved, adequate results of laboratory experiments are only obtained if the experimental conditions can be compared to the real world. If we think of a reaction involving all molecules covering the surface of aerosol particles of 0.1 μm in diameter typically present in 1 m^3 of air, about 10^{-9} Moles are processed. This means that only the most sensitive analytical techniques can be used in experiments performed at atmospheric concentrations of the trace gas involved. In many cases, reactions are affected by physical or chemical interactions of other species not directly involved in the reaction itself. For instance, water adsorbed on solid particles or partially dissolving highly soluble species on or within particles may be a key component in the reactivity of aerosol constituents with trace gases [3]. However, many of the very sensitive and highly specific analytical tools interfere with the presence of water either due its high vapour pressure with respect to vacuum systems or due to its strong absorption in the infrared imposing problems when IR spectroscopy methods are used.

While many experimental techniques have been developed and continue to be further improved in view of the many problems, as shortly addressed above [2], it turns out that the use of short-lived radioactive isotopes may be an exceptionally ideal tool for studying heterogeneous reactions in the laboratory [4]. Especially those radionuclides, which decay by emission of γ-rays, are ideal for studying the exchange of molecules with surfaces in complex environments. Among these, positron emitters have been widely used to trace labelled molecules in space and time, such as in positron emission tomography (PET), *e.g.*, in medical applications. To our knowledge, only very few studies have used short-lived radioactive tracers for gas-solid or gas-liquid interactions. As an example, the spatial distribution of intermediates and products during catalytic conversions has been obtained using the positron emitting nuclides ^{11}C, ^{15}O and to some extent ^{13}N [5]. The advantage of using short-lived nuclides is the very high activity to concentration ratio so that reactions or adsorption may be studied at arbitrarily low concentrations, provided that the tracer is available in at least almost carrier free form. These features allow experiments, *e.g.* with aerosol particles in air suspension at humidity comparable to the real atmosphere. The disadvantage is that chemical information about reactant and products must be obtained by radiochemical separations and has to be checked by conventional methods.

The use of ^{13}N in tracer studies is not so widespread as is the case for ^{11}C. Parks *et al.* [6] suggested to use the reaction $^{16}O(p,\alpha)^{13}N$ in a high pressure oxygen target to produce

*E-mail: markus.ammann@psi.ch

^{13}N-labelled atmospheric nitrogen species. Sajjad *et al.* [7] investigated the excitation function of this reaction in more detail. Routine production of ^{13}N has been implemented in many PET facilities.

During the past ten years, a facility for the on-line production of ^{13}N labelled oxidised nitrogen compounds has been implemented at Paul Scherrer Institute [8]. Oxidised nitrogen compounds and their surface chemical reactions have been of interest in atmospheric chemistry and environmental technology. ^{13}N ($T_{1/2} = 10$ min) has been produced *via* the reaction $^{16}O(p,\alpha)^{13}N$ in a gas-target irradiated by 11 MeV protons and continuously delivered to the laboratory in the form of ^{13}NO. To date, ^{13}N-labelled NO_2, HNO_2, HNO_3, have been synthesised and applied in various experiments pertaining to surface catalysis [8, 9], aerosol science [10], plant physiology [11], and heterogeneous atmospheric chemistry [4, 12, 13].

The applications pertaining to atmospheric chemistry require a continuous and stable source of ^{13}N. Due to the short lifetime of ^{13}N, most experiments have been performed on-line which also means that all labelled species must have been produced from the primary species, ^{13}NO, in continuously working procedures. In the following, an improved target and flow-system setup for ^{13}NO production is described which resulted from the applications mentioned above. Some attention will be given to the synthesis and radiochemical separation of nitrogen oxide molecules of practical interest. A newly developed system to separate and detect gas- phase as well as particulate labelled nitrogen oxide species is described. In a second part, the application of these techniques will be described in two selected experiments of atmospheric interest.

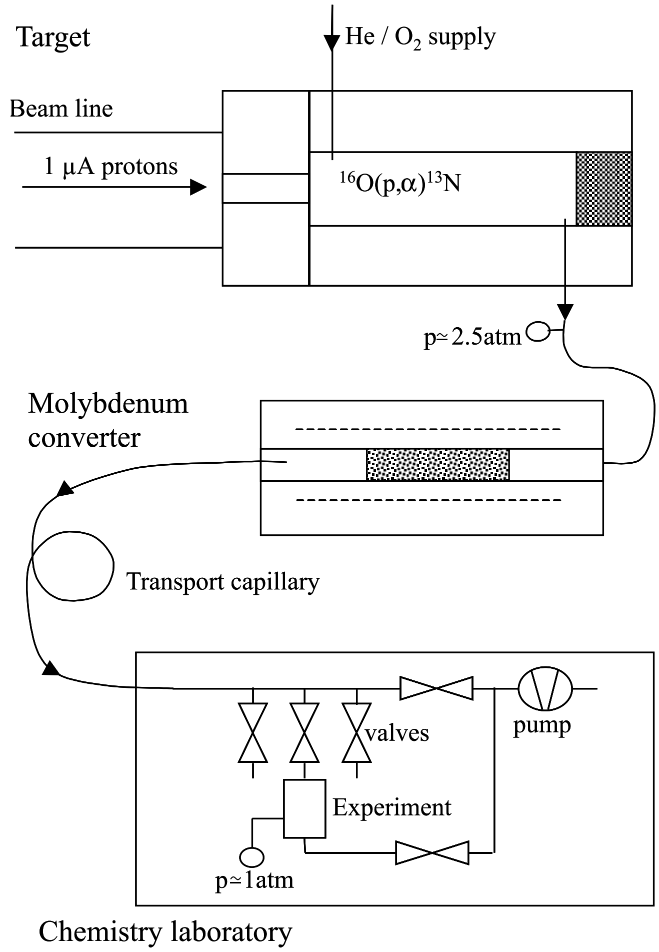

Fig. 1. The ^{13}N production and delivery system consisted of the target, the molybdenum converter, the transport capillary, and the distribution valves in the laboratory. The pressure was kept constant by a pressure regulator mounted at the He/O_2 supply. The drawing of the target also shows the collimator between the gas-target and the beam-line to facilitate beam adjustment.

2. Experimental

Fig. 1 gives an overview of the overall flow scheme used. ^{13}N ($T_{1/2} = 10$ min) was produced *via* the reaction $^{16}O(p,\alpha)^{13}N$ in a gas-target by irradiating ^{16}O with 11 MeV protons. At this energy, the cross-section of this reaction is 55 mb [7]. The target itself consisted of a quartz cylinder (3.6 cm inner diameter) in an aluminium housing, which could be attached to the low-energy beamline of the Philips Cyclotron at Paul Scherrer Institute. The entrance and exit windows consisted of aluminium (0.02 cm thickness). Behind the exit windows, a graphite block was used as beam stop. The housing was isolated to allow control of the beam intensity on the target. The target was kept at a pressure of 2.5 bar and continuously flushed with 10 to 20% O_2 (99.9995%) in He (99.9999%) as carrier gas with a total flow rate of 5 $cm^3 s^{-1}$ STP. The proton energy of the beam was adjusted to 12.8 MeV, with typically 1 μA intensity. Considering the energy loss in the Al window of 1.6 MeV and in the target gas of 0.016 MeV/cm, the proton energy in the middle of the gas target was expected to be 11.1 MeV.

It was expected and confirmed in preliminary experiments that under the influence of radiation chemistry in the gas target, ^{13}N rapidly forms highly oxidized and reactive forms of nitrogen oxides. Because these were presumably affected by wall losses and not favourable for long-distance transport through gas-capillaries, they were chemically converted to ^{13}NO over molybdenum at 500 °C. A quartz tube (0.8 cm i.d.) was filled with 5.5 g of small chips of 0.02 cm thick Mo foil and placed into a tube furnace. The gas target was connected to the tube furnace by 5 m of 0.2 cm i.d. polyethylene tubing. This conversion of primary ^{13}N species to ^{13}NO was key to achieving high overall ^{13}N yields in the laboratory. The same tube was used to transport the resulting gas-mixture to the 80 m distant laboratory (Fig. 1). The transport capillary and the target were additionally contained in a larger tube and a glove box, respectively, which was kept at a pressure slightly below ambient and flushed by Ar (99.998%) to minimise diffusion of impurities through the polyethylene tube walls into the gas going to and coming from the target.

In the laboratory, the gas mixture coming from the target area containing ^{13}NO was passing a NaI detector on which the amount of ^{13}N-labelled molecules passing by per second was determined on-line during the experiments. A 45 cm long 0.4 cm i.d. polyethylene tube was coiled around the cylindrical NaI detector head 7.5 cm in diameter. The efficiency of this configuration was calibrated prior to the experiments by filling the tube with a known amount of ^{18}F in aqueous solution and measuring the resulting counting rate at 511 keV on the detector. Both, ^{13}N and ^{18}F decay through positron emission leading to 511 keV annihilation γ-radiation. After this ^{13}N flow monitor, the gas was fed into up to three experiments by means of three calibrated mass flow controllers (Fig. 1). A fourth mass flow controller was used to maintain the constant overall mass flow rate through the target and gas capillary. This allowed simultaneously operating three independent on-line experiments each with an adjustable fraction of the amount of ^{13}NO available.

^{13}NO was oxidized to $^{13}NO_2$ by reacting it with O_3 in a small flow reactor. Typically 0.5 $cm^3\,s^{-1}$ of the target gas was diluted with synthetic air or N_2 to 8.3 $cm^3\,s^{-1}$. In most experiments carrier ^{14}NO (the presence of the stable isotope ^{15}N is not mentioned any further throughout the paper) was added from a certified cylinder containing 1 ppm NO in N_2 using a calibrated mass flow controller to give total NO concentrations of 0.1 to 100 ppbv (10^9 to 10^{12} cm^{-3}). A small flow of synthetic air was passed through a quartz tube irradiated by a Xe excimer lamp delivering UV light at 172 nm, which results in the formation of O_3. The two gas flows were mixed in the flow reactor of 1000 cm^3 volume. By varying the light intensity, the O_3 concentration could be adjusted to the concentration of NO, so that no O_3 was left after complete oxidation of NO to NO_2 in the flow reactor. The second method to produce ^{13}N-labelled NO_2 was based on the oxidation of NO over solid CrO_3 [14]. In this case, the target gas was diluted as before and then humidified by passing the gas flow through a vertically mounted 0.5 cm i.d. porous Teflon tube partially immersed in water. By varying the water level, the resulting humidity measured by a capacitance humidity sensor could be adjusted to between 30 and 70% relative humidity at ambient temperature. The CrO_3 surface was prepared by immersing firebrick granules 0.4 cm in diameter into a 17% aqueous CrO_3 solution and drying at 105 °C in air. Before use, the granules were exposed to ambient air for 24 hours for conditioning. The humidified gas flow passed over the CrO_3 on firebrick support in a small glass cylinder resulting in complete conversion of NO to NO_2. If the experiment required $^{13}NO_2$ in dry air, the first method was used, whereas in most other experiments, the second method was used.

HNO_2 was produced by reaction of NO_2 with *n*-(1-naphtyl)diethylenediamine-dihydrochloride (NDA). This compound forms part of the Saltzman method to determine the NO_2 concentration in a gas by scrubbing it into an acidic solution and photometrical detection of the resulting nitrite [15]. A glass fiber filter was impregnated with 100 μl of a solution of 1% NDA and 10% water in methanol and dried in N_2. Passing ^{13}N labelled NO_2 in air at 30% relative humidity over this impregnated filter resulted in nearly complete conversion of NO_2 to HNO_2 during a reasonable time period; however, the filters had to be frequently exchanged for longer experiments.

HNO_3 was produced through reaction of NO_2 with OH radicals. NO_2 in dry N_2 (containing about 1% O_2 from O_3 production for NO to NO_2 oxidation) was humidified to between 5 and 25% relative humidity by passing the gas flow through a 2 cm long 0.5 cm i.d. porous Teflon tube completely immersed in water contained in a small glass container. In contrast to the humidifier mentioned above, this container was immersed in a thermo stated alcohol bath adjustable between −20 and +30 °C to obtain a lower range of humidity. The resulting gas flow then passed through a 0.8 cm i.d. quartz tube irradiated with 172 nm UV light. At this wavelength, photolysis of the $H_2O/O_2/N_2$ mixture leads to OH and HO_2 radicals as well as O_3, the concentration of each of which depends on humidity, O_2 content and light intensity [16]. Photolysis of NO_2 is not important compared to the rate of reaction with OH under the conditions adopted here. This configuration resulted in an about 70 to 90% conversion of NO_2 to HNO_3 which was controlled in all experiments by switching the UV lamp on and off, and observing both NO_2 and HNO_3. The conversion efficiency depended mainly on the light intensity, and less on the humidity, because the reaction of NO_2 with OH was presumably limited by the short lifetime of OH in the small flow tube.

Chemical information on the labelled molecules was obtained from sequential separations over specifically coated surfaces. The traps exposing these surfaces were designed as cylindrical or parallel plate denuders that additionally allowed separating gas phase from particulate species [17]. In a denuder, the gas passes with a laminar flow profile and molecules capable of being taken up on the coated wall are absorbed on the wall controlled by lateral diffusion [18]. On the other hand, due to their much lower diffusion coefficients, particles penetrate the denuders with close to 100% efficiency with small losses being mainly caused by impaction in the turbulent entrance zone. The denuder coatings were partially adopted from analogous solutions for the separation and analysis of nitrous gases in the environment [19–21]. For HNO_3, the denuder walls were first wetted with a saturated solution of NaCl in methanol and then dried in N_2. For HONO, the denuder walls were first wetted with a 1.4% solution of Na_2CO_3 in 50% methanol/water and subsequently dried in N_2. Prior to use, this denuder was conditioned by exposing it to 100 ppb NO_2 in air at 30% relative humidity for about 1 hour. It could then be used during several days. For NO_2, the coating solution consisted of 1% NDA, 1% KOH and 10% water in methanol solution, again dried in N_2. For NO, a saturated aqueous solution of $Co(NO_3)_2$ was applied on the denuder surface, which was then first dried in air at 70° and afterwards baked in O_2 for 1 minute at 700 °C. At NO concentrations in the ppb range, this denuder quantitatively absorbs NO for about 8 hours. To regenerate the surface, the denuder was heated to 380 °C for 1 hour to desorb the trapped NO_x species. If the denuders described above were used in this sequence, the assignment of molecules absorbed in each denuder is specific, *i.e.*, HNO_3, HONO, NO_2, and NO, respectively. Particulate ^{13}N species, if applicable, were measured by mounting a glass fiber filter at the end of the denuder line.

In conjunction with a reproducible and efficient detection of ^{13}N labelled molecules trapped in the denuders or the filter, several geometric configurations had been evaluated. Previous experiments had used cylindrical glass denuders coiled around cylindrical NaI detector heads as described in [12, 13]. The disadvantage of this system with one detector for each denuder was that the detection efficiency had to be determined for each individual denuder with an inherent error resulting in a not very high mass balance quality when in an experiment one species was converted to another. Therefore, the system described in the following was de-

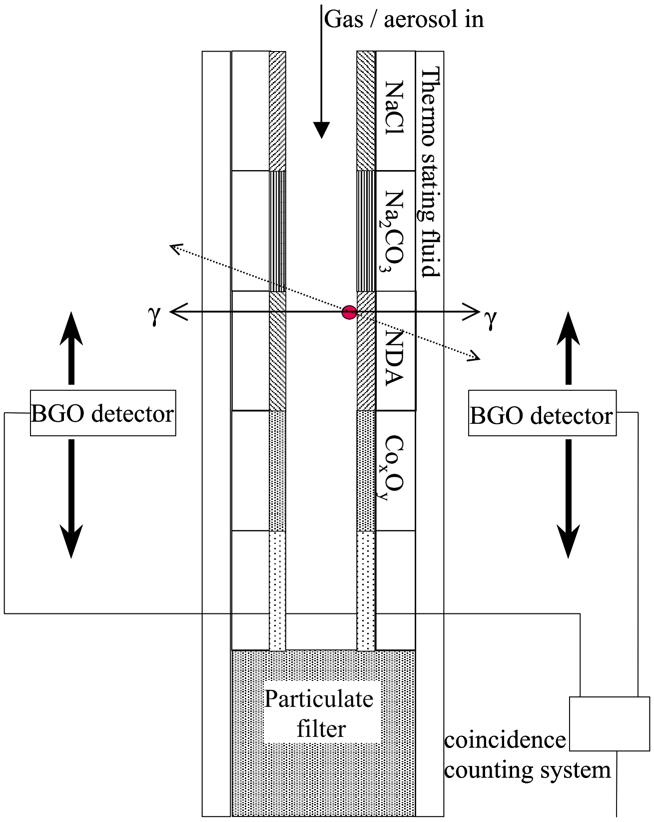

Fig. 2. In the denuder and detection system, gas-phase species are absorbed on the specifically coated denuder plates by diffusion, whereas particles penetrate with nearly 100% efficiency to the particle filter. The coincident counting configuration allows quasi-online measurement of the activity distribution on the denuder plates, or on chromatographic columns (not shown).

veloped, which allowed detection of the activity at all denuders with identical efficiency. This system, shown in Fig. 2, was essentially a narrow, 60 cm long flow tube with a rectangular cross section (inner dimensions $0.1\,\text{cm} \times 2.6\,\text{cm}$). The denuder walls consisted of 5 pairs of 12 cm long aluminium plates (0.2 cm thick) separated by small Teflon liners on both sides. The plates were mounted into an aluminium housing which included a jacket for thermostating as well as an inlet designed to allow the laminar flow profile to be rapidly established. For each experiment, the denuder plates were coated according to the specific requirements. In the denuder mode, this system was used to separate gas phase from particulate nitrogen oxide species. In the flow tube mode, the first plate was used as substrate for a reactive material exposed to labelled NO_2, and the following plates were used to analyse the products. In both cases, this parallel plate flow tube/denuder system was mounted onto a linear motion device on which a stepper motor was used to move a pair of BGO-detector heads (3 cm in diameter) mounted face to face with a gap of 3.5 cm along the denuder system. The annihilation of the positron emitted in the decay of ^{13}N leads to emission of two coincident γ rays in opposite directions. Therefore, the output of each detector operated at 800 V was wired to a timing filter amplifier and constant fraction discriminator, and combined to a coincident counting unit with a logical ‘and’ unit. This allowed the determination of the spatial distribution of ^{13}N along the denuder system or thermochromatography columns with very low background noise. The device was moved continuously along these columns or denuders, and counts were integrated and recorded with a resolution of 0.5 cm. The system was calibrated by coating one of the denuder plates with a known amount of a calibrated aqueous ^{18}F solution, before the experiments were started.

Parallel to the radiochemical separation and detection, total nitrogen oxide concentrations were determined in all experiments using commercial NO_x chemiluminescence analysers giving NO and NO_2 concentrations in their standard configuration. More details about the nitrogen oxides measurement are given in [13]. Ozone concentrations were determined using a commercial ozone analyser using a UV absorption technique.

3. Results and discussion

3.1 Performance of ^{13}N production

The system as described above had been continuously developed and improved during several beam-times since 1991. Typical beam time periods lasted about 120 hours. At the start of each beam time, the half-life of the nuclides transported to the laboratory was determined to control the production of ^{13}N. For this purpose, the gas flow coming from the target was accumulated on the denuder specific for NO for about 1 hour, and decay of the activity was observed during another 2 hours. The average half-life obtained was 10.11 ± 0.20 min, close to the published value of 9.97 min [22]. Several unsuccessful attempts were made to accumulate activity and observe its decay over longer time-scales to assess any contribution of ^{18}F with a half-life of 110 min [22]. Although the cross section of the reaction $^{18}O(p,n)^{18}F$ is about 150 mb at 12 MeV [23], the contribution of this reaction to the observed activity remained low because the fraction of ^{18}O in the irradiated O_2 was only 0.2%. When the molybdenum converter heating close to the target was switched off, which resulted in an efficient absorption of all nitrogen oxides on Mo, a very small amount of activity could be trapped in the basic denuder for NO_2 absorption, with a half-life of 20 min. This activity was attributed to ^{11}C [22], which was presumably transported in the form of $^{11}CO_2$, being able to pass the Mo converter at room temperature. Under the conditions in our target, the contribution of the reactions $^{16}O(p,\alpha pn)^{11}C$ (cross section < 1 mb at 11 MeV [23]) to the production of ^{11}C should be negligible. Instead, the main source of ^{11}C seemed to be the reaction $^{14}N(p,\alpha)^{11}C$ (cross section 126 mb at 12 MeV, [24]) from N_2 impurities present in the gas supplies. The fraction of ^{11}C in the product gas was always less then 0.1% as determined from chemical separation experiments not shown here, and also during the application experiments, in none of the traps any significant ^{11}C activity was observed. Several more experiments with the Mo converter showed that the maximum ^{13}NO yield was obtained at 500 °C. This was an indication that the most prominent stable species formed in and after the target was a higher oxide of nitrogen than NO_2, because NO_2 and HONO are already reduced to NO over Mo at 350 °C [25]. From earlier thermochromatographic studies of products from a similar target and without a Mo converter in line [9] it was concluded that

HNO_3 might be the dominant species, and the experiments by Parks using a high purity high pressure O_2 gas target also indicated the presence of HNO_3. It is likely that OH, O and HO_2 radicals and O_3 were formed in the target gas under proton irradiation. These radicals might then combine with NO, NO_2 or other unstable intermediate species to form $H^{13}NO_3$.

Based on the cross section of the $^{16}O(p,\alpha)^{13}N$ reaction of 55 mb [7] at 11 MeV, a production rate of $5 \times 10^7\ s^{-1}$ is expected at 1 μA proton current. From the activity measurements with the calibrated target gas monitor in the laboratory at the end of the transport capillary, a ^{13}N flux of typically $10^7\ s^{-1}$ was derived, corresponding to an activity of about $2 \times 10^3\ Bq\,cm^{-3}$. It usually increased slightly during the first 12 hours and remained constant at this level afterwards. The initial slow increase was ascribed to a passivation of the surfaces to which $H^{13}NO_3$ is exposed in and behind the target. The production rate depended linearly on the oxygen content in the target gas and on the beam current. The estimated overall transport yield of about 20% seemed reasonable when considering the 5 m long polyethylene tubing between the gas target and the Mo converter and the fact that HNO_3 exhibits significant retention along most surfaces [26]. This transport yield was remarkably constant over many beam times. As the presence of ^{11}C was an indication of $^{14}N_2$ impurity in the irradiated gas mixture, it is also not surprising that ^{14}N oxide species were formed in this system providing a source of carrier NO (after reduction in the Mo converter). The concentrations of NO in the target gas measured by the chemiluminescence detector reached about 30 ppbv, which was lower than the levels observed by Parks. However, in that study, the proton beam intensities were higher (10 μA), and the N_2 impurity levels might have been different. The amount of carrier NO was also reproducible and did not significantly depend on the individual gas cylinders used to supply He and O_2. However, whereas the production rate increased with the oxygen content, the amount of carrier NO decreased (Fig. 3). The reason for this is not clear: if the main source of N_2 in the system was not an impurity associated with the O_2 supply, it seems that oxygen was quenching in some way the radical reactions leading to oxidised nitrogen compounds. For the applications in atmospheric chemistry, where low NO_x concentrations were required, the system was operated as described in the experimental part, *i.e.* 20% O_2 in He, giving higher $^{13}N/^{14}N$ ratios.

The performance of the ^{13}N production facility was remarkably constant and reproducible with respect to transport yield, carrier NO content and stability over several beamtimes. This was a prerequisite for a successful development of the experimental approaches detailed below.

3.2 Applications

3.2.1 Reversible adsorption of NO_2 on NaCl

In the atmosphere, NaCl is the main constituent of sea salt aerosol generated *via* sea spray on the oceans and representing a very important aerosol material of the troposphere. Heterogeneous processes involving nitrogen oxides are slowly depleting chloride in the sea salt aerosol by forming nitrates on the aerosol and HCl in the gas-phase. Several studies have also addressed the reaction of NO_2 with sea salt and NaCl alone (*e.g.*, [3]). In the example shown here, the interaction of $^{13}NO_2$ with NaCl was investigated using thermo chromatography, a technique described in more detail by Eichler *et al.* [27], in which the surface material of interest configured as stationary phase of a chromatography column is exposed to a temperature gradient, while a carrier gas is continuously passing the column. For this experiment (shown in Fig. 4), a smooth and transparent NaCl film was prepared by wetting a 4 mm i.d. quartz tube with molten NaCl at 800 °C and subsequent cooling at a slow rate. $^{13}NO_2$ in air as carrier gas was fed to this NaCl column in the temperature gradient (300 K to 80 K) during 30 min. The column was then removed from the apparatus, immersed in liquid nitrogen, before the activity distribution along the column was measured. The symmetric peak shown in Fig. 4 confirmed that reversible adsorption was the main process governing migration of $^{13}NO_2$ along the NaCl surface. For this particular experiment, an adsorption enthalpy

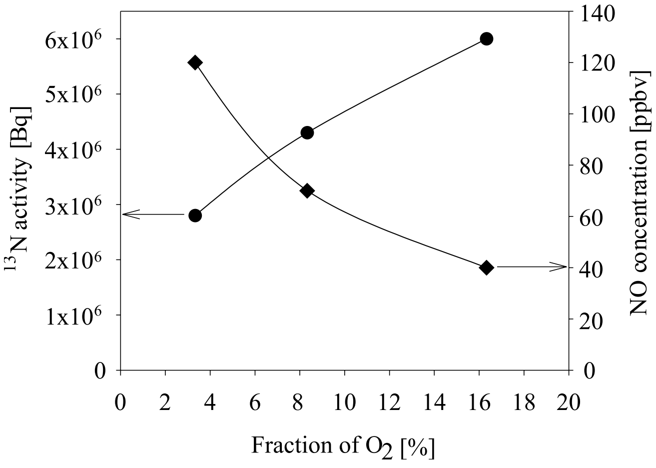

Fig. 3. The ^{13}N activity transported to the laboratory (circles, left) and the carrier NO concentration (diamonds, right) is plotted against the fraction of O_2 in the carrier gas passing the target at 1 μA 11 MeV protons.

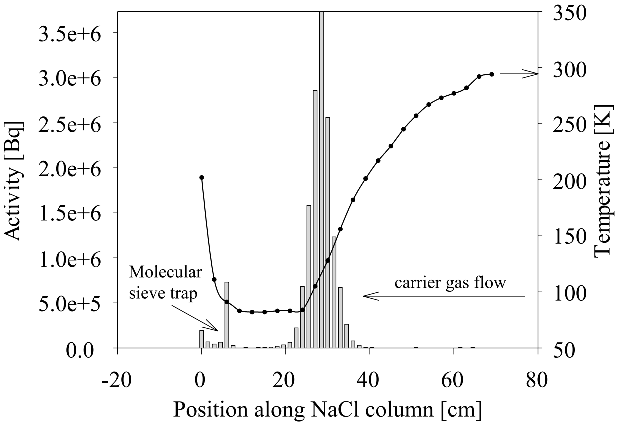

Fig. 4. In this thermochromatography experiment, a quartz column coated with NaCl was exposed to a flow containing $^{13}NO_2$ in a temperature gradient (solid line, right axis), with the gas flowing from the warm to the cold end. After the experiment, the activity distribution was measured (bars, left axis). A molecular sieve trap at the end of the coating was used to trap all ^{13}N species not retained in the column.

of 28 kJ mol^{-1} was derived based on an evaluation procedure as described in detail by Eichler *et al*. [27]. The experiment also allowed estimating an upper limit to the reaction probability, γ, of NO_2 with NaCl, which is defined as the fraction of total gas kinetic collisions of NO_2 with the surface that result in irreversible loss on the surface. This would lead to a homogeneous distribution of activity along the NaCl surface. From the small amount of activity (not visible in Fig. 4) accumulated between the entrance of the NaCl column and before the peak assigned to reversible adsorption, γ was estimated to be about 5×10^{-8} in the temperature range from 200 to 300 K. This is the collision-based probability that a surface nitrate is formed from NO_2. This is a very slow process and is not very effective in converting NaCl into $NaNO_3$. However, in the atmosphere, on real sea-salt particles and with higher humidity and other constituents, the reactivity may significantly increase [3]. Nevertheless, the experiment shown provides a very powerful means of addressing reversible and irreversible processes at the same time. The method is also directly applicable to a realistic sea salt surface prepared from ocean water, or any other surface of atmospheric interest, *e.g*., ice [28].

3.2.2 Reaction of HNO_3 with sea salt aerosol particles

The most important process removing nitrogen oxides from the atmosphere is the oxidation of NO_2 by OH radicals and subsequent scavenging and deposition of HNO_3 by aerosol particles, rain and snow. Thereby, the uptake of HNO_3 on aerosol particles is a key process [29], and the kinetics has not been well established for atmospheric aerosol particles. In addition, in contrast to the reaction of NO_2, the reaction of HNO_3 with sea-salt is indeed very effective in converting sea-salt chloride into nitrate.

For the experiment presented here, a small flow reactor consisting of a 0.8 cm i.d. Teflon tube was attached in front of the denuder and detection system (Fig. 2). At the entrance of this tube, a flow containing sea salt aerosol particles was mixed with the flow containing ^{13}N labelled HNO_3. The aerosol was generated from nebulising a synthetic aqueous sea salt solution in air. Aerosol conditioning and characterisation are described in detail in [13]. The particle size distribution was lognormal with a maximum at about 150 nm. The particle generation could be switched on and off, without affecting the flow rates. The length of the flow reactor determined the interaction time between HNO_3 and the aerosol of typically between 0.2 s and 2 s.

During the experiment, the activity distribution along the denuder system was scanned every three minutes. Fig. 5 shows scans recorded during a typical experiment and also the distribution of the denuder coatings used. The experiments were started with the UV lamp to convert NO_2 into HNO_3 switched off, and the activity is concentrated on the coating specific for NO_2. In these experiments, also some O_3 was present leading to a more rapid deactivation of this coating, so that the NO_2 peak was relatively broad and moved slowly along the plate with time. The coating was replaced frequently enough to avoid any losses.

After about 30 min, the UV lamp was switched on, converting nearly all NO_2 to HNO_3, leading to an increase

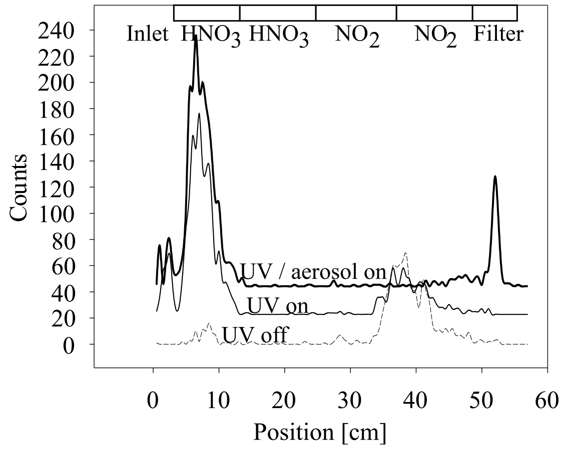

Fig. 5. During the HNO_3-aerosol experiments, the denuder system was continuously scanned to derive the amount of ^{13}N associated with each species absorbed on the plates as indicated on the upper horizontal axis. The lower curve shows the distribution for NO_2 alone, the middle curve after the UV lamp had been switched on to convert NO_2 into HNO_3, and the upper curve after the aerosol had been switched on.

of activity on the coating specific for HNO_3 and a decrease where NO_2 was absorbed before (middle curve in Fig. 5). The width of the HNO_3 activity peak was consistent with removal of HNO_3 from the gas-phase controlled by diffusion: for the present geometry and volumetric gas flow rates, more than 95% of the HNO_3 molecules should have reached the wall within a length of 3 cm along the denuder plates, assuming that every molecule hitting the wall was taken up [17]. This diffusion controlled transport to the denuder plates also defines the characteristic time of exposure of $HNO_3(g)$ to the particles after the end of the flow reactor of around 30 ms, which was added to the interaction time given by the geometry of the flow reactor.

Another 30 min later, the aerosol was switched on. The activity at the position of the particle filter increased (upper curve in Fig. 5) whereas the activity associated with gas-phase HNO_3 decreased. The changes in both signals are the signatures of the reaction proceeding in the flow reactor.

For an experiment as shown, the integrals of the peaks for each species, j, were calculated for each scan, i, performed every 3 min. From the difference of two consecutive activity measurements, i and $(i-1)$, the saturating activity, A_j, which is equal to the total amount of ^{13}N-labelled molecules being absorbed at its specific denuder plate per unit time, was calculated for each species using

$$A_j = \frac{\alpha_{ij} - \alpha_{(i-1)j}\,\mathrm{e}^{-\lambda \Delta t_i}}{1 - \mathrm{e}^{-\lambda \Delta t_i}}\,,$$

where α_{ij} is the activity (radioactive decays per second) at time t_i for species j and $\Delta t_i = t_i - t_{(i-1)}$. λ is the decay constant of ^{13}N ($\lambda = 0.00116\ \mathrm{s}^{-1}$). Fig. 6 shows the result of this data evaluation for a typical experiment, clearly showing the sharp changes associated with switching on the UV light and the aerosol particles, respectively. Assuming negligible kinetic isotope effects, the activities as displayed can be converted to the total concentration of each species, *i.e*., the concentration of labelled and non-labelled molecules, by correcting for the volumetric gas flow rate and the ratio of labelled to non-labelled molecules. This ratio

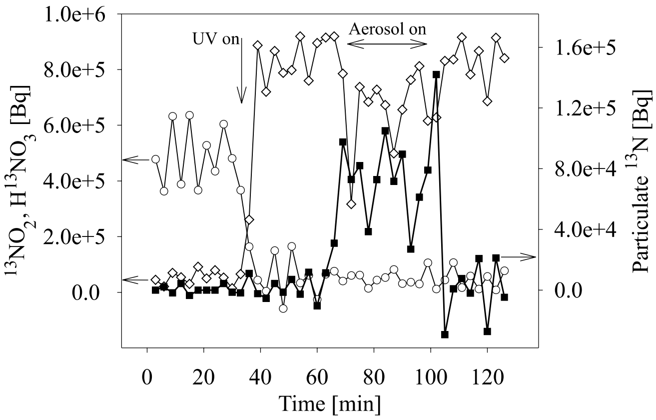

Fig. 6. From two consecutive measurements of the activity associated with each species on the denuder system, the saturating activities for each species was derived as shown in the text and plotted as a function of the time during the experiment. The figure indicates the effect of switching on the UV lamp on to convert NO_2 (open circles, left axis) into HNO_3 (open diamonds, left axis) and of switching on the aerosol to form particulate ^{13}N species (solid squares, right axis) due to the reaction of HNO_3 with the particles in the flow reactor.

was derived from the activity associated with $^{13}NO_2$ on the denuder and the measurement of NO_2 with the chemiluminescence detector sampling from the gas prior to entering the UV lamp and the flow reactor. In the case shown in Fig. 6, the initial NO_2 concentration was 1.55×10^{11} cm^{-3} (6.3 ppb), so that the ratio of labelled to non-labelled molecules was 4.6×10^{-7}. From that, a HNO_3 concentration of 1.40×10^{11} cm^{-3} (5.7 ppb) was derived. The concentration of particulate species derived from the reaction (presumably surface nitrate) was 2.80×10^{10} cm^{-3} (11.4 ppb), which was about 20% of HNO_3(g) admitted to the flow reactor. In this particular experiment, the aerosol surface to volume ratio was 1.67×10^{-4} cm^2 cm^{-3}, so that the amount of products on the aerosol surface was 1.40×10^{14} cm^{-2}. This was clearly below a formal monolayer, so that second-order or saturation effects did not affect the result.

Considering the effective length of the flow reactor of 16 cm for the experiment shown, the actual aerosol-HNO_3(g) interaction time was 0.89 s. A mass transfer calculation as described in [30] was used to calculate the reaction probability, γ, which is the probability that a collision of HNO_3(g) results in irreversible uptake onto the particles. This calculation takes into account the size distribution of the aerosol, gas-phase diffusion of HNO_3, and classical gas-kinetic theory to calculate the collision frequency. A value of $\gamma = 0.07$ was derived from several measurements like that shown in Fig. 6. This value lies in the range to be expected from studies on bulk NaCl surfaces [31]. A more detailed discussion of this kinetics, and the implications for the mechanism of HNO_3 uptake to sea-salt aerosol particles is beyond the scope of this paper and will be discussed elsewhere.

This experiment illustrates the capability of the ^{13}N tracer technique for the investigation of gas-aerosol reactions at concentrations where the amount of processed reactants would be too small for most classical analytical tools. The kinetics of these reactions can be observed with a time resolution of below 100 ms, which is sufficient for most problems of atmospheric relevance. The detection limits are not affected by the most important environmental parameters in these systems, *i.e.*, pressure, temperature, and humidity.

Acknowledgment. This work has been initiated by many preliminary experiments performed by H. W. Gäggeler, U. Bochert, U. Baltensperger, M. Kalberer, D. T. Jost, A. Türler, F. Arens. B. Eichler and P. Zimmermann provided the NaCl coated quartz tube and the thermochromatography setup. D. Piguet and E. Rössler provided valuable technical support. The stable proton beams over many days and nights provided by the staff of the PSI Accelerator Facilities are greatly appreciated. This work was supported by the Swiss National Science Foundation, the Swiss Federal Government of Education and Science, and the Kommission für Technologie und Innovation.

References

1. Jacob, D. J.: Heterogeneous chemistry and tropospheric ozone. Atmos. Environ. **34**, 2131 (2000).
2. Ravishankara, A. R.: Heterogeneous and multiphase chemistry in the troposphere. Science **276**, 1058 (1997).
3. Langer, S., Pemberton, R. S., Finlayson-Pitts, B.: Diffuse reflectance infrared studies of the reaction of synthetic sea salt mixtures with NO_2: a key role for hydrates in the kinetics and mechanism. J. Phys. Chem. A **101**, 1277 (1997).
4. Ammann, M., Kalberer, K., Jost, D. T., Tobler, L., Rössler, E., Piguet, D., Gäggeler, H. W., Baltensperger, U.: Heterogeneous production of nitrous acid on soot in polluted air masses. Nature **395**, 157 (1998).
5. Jonkers, G., Vonkeman, K. A., van der Wal, S. W. A., van Santen, R. A.: Surface catalysis studied by in situ positron emission. Nature **355**, 63 (1992).
6. Parks, N. J., Peek, N. F., Goldstein, E.: The synthesis of ^{13}N labeled atmospheric gases *via* proton irradiation of a high pressure oxygen target. Int. J. Appl. Rad. Isotopes **26**, 683 (1975).
7. Sajjad, M., Lambrecht, R. M., Wolf, A. P.: Cyclotron isotopes and radiopharmaceuticals. XXXVII. Excitation functions for the $^{16}O(p, a)^{13}N$ and $^{14}N(p, pn)^{13}N$ reactions. Radiochim. Acta **39**, 165 (1986).
8. Baltensperger, U., Ammann, M., Bochert, U. K., Eichler, B., Gäggeler, H. W., Jost, D. T., Kovacs, J. A., Türler, A., Scherer, U. W., Baiker, A.: Use of positron-emitting ^{13}N for studies of the selective reduction of NO by NH_3 over vanadia/titania catalyst at very low reactant concentrations. J. Phys. Chem. **97**, 12 325 (1993).
9. Eichler, B., Baltensperger, U., Ammann, M., Jost, D. T., Gäggeler, H. W., Türler, A.: Thermochromatographic investigation of ^{13}N labelled nitrous gases and of fission noble gases at low temperatures. Radiochim. Acta **68**, 41 (1995).
10. Ammann, M., Baltensperger, U., Bochert, U. K., Eichler, B., Gäggeler, H. W., Jost, D. T., Türler, A., Weber, A. P.: Study of HI, HBr and NO_2 adsorption on graphite and silver aerosol particles using short- lived isotopes. J. Aerosol Sci. **26**, 61 (1995).
11. Ammann, M., Stalder, M., Brunold, C., Baltensperger, U., Jost, D. T., Türler, A.,Gäggeler, H. W.: Tracing uptake and assimilation of NO_2 in spruce needles with ^{13}N. J. Exp. Bot. **46**, 1685 (1995).
12. Kalberer, M., Tabor, K., Ammann, M., Parrat, Y., Weingartner, E., Piguet, D., Rössler, E., Jost, D. T., Türler, A., Gäggeler, H. W., Baltensperger, U.: Heterogeneous chemical processing of $^{13}NO_2$ by monodisperse carbon aerosols at very low concentrations. J. Phys. Chem. **100**, 15 487 (1996).
13. Kalberer, M., Ammann, M., Arens, F., Gäggeler, H. W., Baltensperger, U.: Heterogeneous formation of nitrous acid (HONO) on soot aerosol particles. J. Geophys. Res. **104**, 13 825 (1999).
14. Levaggi, D., Siu, W., Feldstein, M., Kothny, E. L.: Quantitative separation of nitric oxide from nitrogen dioxide at atmospheric concentration ranges. Environ. Sci. Technol. **6**, 250 (1972).
15. Saltzman, B. E.: Colorimetric microdetermination of nitrogen dioxide in the atmosphere. Anal. Chem. **26**, 1948 (1954).
16. Aschmutat, U., Hessling, M., Holland, F., Hofzumahaus, A.: A tunable source of hydroxyl (OH) and hydroperoxy (HO_2) radicals: in the range between 10^6 and 10^9 cm^{-3}. In: *Physico-chemical behaviour of atmospheric pollutants*. (Angeletti, G., Restelli, G. Eds.) European Commission, Luxembourg (1994).

17. Willeke, K., Baron, P. A.: *Aerosol Measurement Principles, Techniques, and Applications*. Van Nostrand Reinhold, New York (1993) p. 436.
18. Gormley, P. G., Kennedy, M.: Diffusion from a stream flowing through a cylindrical tube. Proc. Royal Irish Acad. 163 (1949).
19. Allegrini, I., Santis, F. D., Palo, V. D., Febo, A., Perrino, C., Possanzini, M.,Liberti, A.: Annular denuder method for sampling reactive gases and aerosols in the atmosphere. Sci. Tot. Environ. **67**, 1 (1987).
20. Williams, E. L., Grosjean, D.: Removal of atmospheric oxidants with annular denuders. Environ. Sci. Technol. **24**, 811 (1990).
21. Braman, R. S., Cantera, M. A. d. l., Han, Q. X.: Sequential, selective hollow tube preconcentration and chemiluminescence analysis system for nitrogen oxide compounds in air. Anal. Chem. **58**, 1537 (1986).
22. Firestone, R. B., Shirley, V. S., Baglin, C. M., Chu, S. Y. F., Zipkin, J. (Eds.): *Table of Isotopes*. Vol. 1, John Wiley & Sons, Inc., New York (1996).
23. Schopper, H.: *Production of Radionuclides at Intermediate Energies, Numerical data and Functional Relationships in Science and Technology*/*Landolt-Börnstein*. Vol. 13 (Hellwege, K.-H. Ed.) Springer, Berlin (1991).
24. Bida, G. T., Ruth, T. J., Wolf, A. P.: Experimentally determined thick target yields for the $^{14}N(p, a)^{11}C$ reaction. Radiochim. Acta **27**, 181 (1980).
25. Roscoe, H. K., Clemitshaw, K. C.: Measurement techniques in gas-phase tropospheric chemistry: a selective view of the past, present, and future. Science **276**, 1065 (1997).
26. Neuman, J. A., Huey, L. G., Ryerson, T. B., Fahey, D. W.: Study of inlet materials for sampling atmospheric nitric acid. Environ. Sci. Technol. **33**, 1133 (1999).
27. Eichler, B., Zvara, I.: Evaluation of the enthalpy of adsorption from thermochromatographical data. Radiochim. Acta **30**, 233 (1982).
28. Eichler, B., Zimmermann, H. P., Gäggeler, H. W.: Adsorption of radon on ice surfaces. J. Phys. Chem. A **104**, 3126 (2000).
29. Dentener, F. J., Crutzen, P. J.: Reaction of N_2O_5 on tropospheric aerosols: impact on the global distributions of NO_x, O_3, and OH. J. Geophys. Res. **98**, 7149 (1993).
30. Rogak, S. N., Baltensperger, U., Flagan, R. C.: Measurement of mass transfer to agglomerate aerosols. Aerosol Sci. Technol. **14**, 447 (1991).
31. Davies, J. A., Cox, R. A.: Kinetics of the heterogeneous reaction of HNO_3 with NaCl: Effect of water vapor. J. Phys. Chem. A **102**, 7631 (1998).